



HAL
open science

Variation of dissolved and particulate metal(loid) (As, Cd, Pb, Sb, Tl, Zn) concentrations under varying discharge during a Mediterranean flood in a former mining watershed, the Gardon River (France)

Eléonore Resongles, Corinne Casiot, Remi Freydieier, Marion Le Gall, Françoise Elbaz-Poulichet

► To cite this version:

Eléonore Resongles, Corinne Casiot, Remi Freydieier, Marion Le Gall, Françoise Elbaz-Poulichet. Variation of dissolved and particulate metal(loid) (As, Cd, Pb, Sb, Tl, Zn) concentrations under varying discharge during a Mediterranean flood in a former mining watershed, the Gardon River (France). *Journal of Geochemical Exploration*, 2015, 158, pp.132–142. 10.1016/j.gexplo.2015.07.010 . hal-02063551

HAL Id: hal-02063551

<https://hal.science/hal-02063551v1>

Submitted on 31 May 2021

HAL is a multi-disciplinary open access archive for the deposit and dissemination of scientific research documents, whether they are published or not. The documents may come from teaching and research institutions in France or abroad, or from public or private research centers.

L'archive ouverte pluridisciplinaire **HAL**, est destinée au dépôt et à la diffusion de documents scientifiques de niveau recherche, publiés ou non, émanant des établissements d'enseignement et de recherche français ou étrangers, des laboratoires publics ou privés.

1 **Variation of dissolved and particulate metal(loid) (As, Cd, Pb, Sb,**
2 **Tl, Zn) concentrations under varying discharge during a**
3 **Mediterranean flood in a former mining watershed, the Gardon**
4 **River (France)**

5 Eléonore Resongles^{a*}, Corinne Casiot^a, Rémi Freydier^a, Marion Le Gall^a and Françoise Elbaz-
6 Poulichet^a

7 ^aHydroSciences UMR 5569, CNRS, Universités Montpellier I & II, IRD, Place Eugène
8 Bataillon, CC MSE, 34095 Montpellier Cedex 5, France

9 *Corresponding author:

10 Tel.: +33467143605

11 E-mail address: eleonore.resongles@univ-montp2.fr

12 ABSTRACT

13 The variation of dissolved and particulate metal(loid) concentrations was investigated
14 during a Mediterranean flood in a former mining watershed, the Gardon River (SE France),
15 using high-temporal resolution sampling.

16 Dissolved antimony originating from the upper Gardon River watershed underwent
17 dilution during flood. Conversely, dissolved As and particulate As, Pb, Zn, Cd and Tl
18 concentrations exhibited increased values during rising flood compared to low and receding
19 flow conditions, with a double-peak shape. As, Pb, Cd and Tl concentration data in suspended
20 particulate matter from this double-peak were distributed along two different correlation lines,
21 showing the successive mobilization of two groups of particles highly enriched with As and
22 Cd or Pb and Tl, both inherited from ancient Pb/Zn mines.

23 Metal(loid) loads during the monitored 24 h-flood event were: 0.5 kg for Cd, 19.4 kg for
24 Sb and 204 kg for As in the dissolved phase and 24 kg for Cd, 38 kg for Tl, 94 kg for Sb,
25 1915 kg for As, 2860 kg for Pb and 5214 kg for Zn in the particulate phase.

26 Altogether, these results highlighted the importance of floods in the mobilization of
27 metals and metalloids from ancient mining sites in Mediterranean regions, showing the need
28 for high-temporal resolution monitoring of flood event to accurately assess the long-term
29 contribution of mining activity to metal(loid) loads of downstream watershed.

30

31

1 KEYWORDS

- 2 Flood event; high temporal resolution sampling; metal and metalloid load; contaminated
3 particles remobilization; mining pollution; Mediterranean watershed

1. Introduction

River systems that drain former mining regions are generally contaminated with metals and metalloids even long after the mining activity has ceased (Macklin et al. 1997; Young 1997; MacKenzie and Pulford 2002; Coulthard and Macklin 2003). This trend is due to the persistence of contamination sources which include untreated mining waters, mining wastes, tailings and smelting slags that remained on sites as well as contaminated sediments stored downstream in riverbeds, floodplains or reservoir lakes (Moore and Luoma 1990; Hudson-Edwards 2003). These mining-related pollutions affect the immediate vicinity of mines but also hydrosystem further downstream (Moore and Luoma 1990; Axtmann and Luoma 1991; Miller et al. 2004, 2007).

In Europe, metal(loid) inputs from former mining sites often represent an obstacle to achieve the good chemical and ecological status of surface waters aimed by the Water Framework Directive (2000/60/EC) (Younger and Wolkersdorfer 2004; Mayes et al. 2009; Mighanetara et al. 2009; Foulds et al. 2014). Assessment of water quality downstream from these former mining sites is generally based on discrete measurements of metal(loid) concentrations during baseflow, on a monthly or weekly basis at best. However, little studies have focused on metal(loid) dynamic during flood events in former mining regions although floods are particularly effective agents of metal(loid) transport in rivers (Bradley 1984; Miller et al. 1999; Dennis et al. 2003; Coynel et al. 2007; Žák et al. 2009; Gozzard et al. 2011; Foulds et al. 2014). This is especially relevant in Mediterranean rivers affected by short and intense floods during which the great part of suspended particulate matter (SPM) and contaminant flux occur (Meybeck 2001; Pont et al. 2002; Cánovas et al. 2008, 2012; David et al. 2012).

Significant variations of metal(loid) concentrations have been recorded in mining-impacted rivers within a single flood event both in dissolved and particulate phases. Metal-contaminated particles enter the river through erosion of mine waste tips and contaminated soils caused by heavy rainfalls (Gao and Bradshaw 1995; Dennis et al. 2003; Hudson-Edwards 2003; Macklin et al. 2006; Gozzard et al. 2011; Byrne et al. 2012) and reworking of historically contaminated sediments containing both primary (e.g. sulfides) and secondary (e.g. Fe and/or Al (oxy)hydroxides) metal-bearing phases (Macklin and Klimek 1992; Macklin et al. 1997, 2006; Coulthard and Macklin 2003; Dennis et al. 2003; Hudson-Edwards 2003; Coynel et al. 2007; Žák et al. 2009; Gozzard et al. 2011; Cánovas et al. 2012; Foulds et

1 al. 2014). Therefore, increasing particulate metal(loid) concentrations in SPM have been
2 reported in relation with increasing discharge in mining-impacted river (Lehmann et al. 1999;
3 Coynel et al. 2007) while the usual trend for particulate metal(loid) concentrations during
4 floods is a decrease due to dilution by less contaminated sediment, change in grain size and
5 exhaustion of available contaminated particles (Bradley and Lewin 1982; Bradley 1984;
6 Dawson and Macklin 1998; Schäfer and Blanc 2002).

7 Furthermore, an increase of dissolved metal(loid) concentrations downstream from old
8 mines has been reported during rising floods and was assigned to flushing of metal-rich
9 soluble secondary sulfates accumulated at mining sites during summer (Grimshaw et al. 1976;
10 Hudson-Edwards et al. 1999; Keith et al. 2001; Cánovas et al. 2008, 2010; Byrne et al. 2013),
11 contribution of contaminated subsurface water or groundwater (Cánovas et al. 2008; Byrne et
12 al. 2013) and metal(loid) release from mineral phases (Byrne et al. 2013).

13 Overall, these studies have highlighted the need to monitor floods with high temporal
14 resolution sampling in order to better understand metal(loid) behavior and fate downstream
15 from mining site under flood conditions. However, flood monitoring studies are scarce and
16 often focused on small watershed at the outlet of a single mining site, only little research was
17 carried out on medium watersheds affected by several contamination sources (Coynel et al.
18 2007; Cánovas et al. 2008, 2012).

19 The aim of this study was to investigate temporal variability of dissolved and particulate
20 metal(loid) concentrations during a Mediterranean flood in a former mining watershed of
21 medium size, the Gardon River watershed (France). For this purpose, spatial surveys of
22 metal(loid) concentrations were carried out during low and high flow. Moreover, high
23 temporal resolution sampling was performed during two consecutive floods at two stations of
24 the Gardon River watershed and SPM, dissolved and particulate metal(loid) concentrations
25 were determined.

1 2. Study area

2 2.1. Geological characteristics and mining legacy of the Upper Gardon River

3 The Gardon River is the most southern tributary of the Rhône River (SE France,
4 Figure 1). The Upper Gardon River is divided into two main sub-basins; the Gardon of
5 Anduze watershed (~627 km²) and the Gardon of Ales watershed (~448 km²); from its
6 headwaters in the Cevennes Mountains to the junction of the two subwatersheds at Ners, the
7 Gardon River has a drainage area of 1100 km² (Figure 1).

8 The Upper Gardon River drains granitic and metamorphic bedrocks belonging to the
9 Paleozoic geological formations of the French Massif Central. The middle and lower parts are
10 underlain by Jurassic (west) to Cretaceous (east) carbonated formations (BRGM, Infoterre
11 website; Resongles et al. 2014).

12 Land occupation on the Upper Gardon River consists mainly in forest, being 76% for
13 the Gardon of Ales subwatershed and 89 % for the Gardon of Anduze subwatershed (Corine
14 Land Cover, 2006). There is also one mid-size town, Ales (~40,000 inhabitants) and a
15 chemical industrial center at Salindres (Figure 1). The Upper Gardon River drains many
16 former mining sites exploited mainly for Pb, Zn, Sb, pyrite and coal. Modern exploitation
17 occurred from the mid-19th century to the end of the 1960s and let large amounts of mining
18 wastes on sites (Table 1). This ancient exploitation has durably enriched the Gardon River
19 sediments with As, Cd, Hg, Pb, Sb, Tl and Zn (Resongles et al. 2014). This enrichment
20 reaches a factor 24 for main stream sediments compared to the local geochemical background
21 and a factor 1849 for mine-impacted tributaries (Aiguesmortes, Amous, Avène, Ourne,
22 Grabieux, Ravin des Bernes, Richaldon) (Resongles et al. 2014).

23 2.2. Hydrological characteristics of the Upper Gardon River

24 The Gardon River is characterized by a Mediterranean hydrological regime i.e. high
25 seasonal variations (Figure 2a). Its mean annual discharge maximum during the studied period
26 (2011-2013) was 26.6 m³/s at Ners, 15.4 m³/s at Anduze and 6.9 m³/s at Ales (Banque Hydro
27 website). Summer flows are very low with mean monthly discharge generally below 3 m³/s at
28 Ners during July and August. In spring and autumn, the Gardon River watershed is affected
29 by flash flood events, with instantaneous discharges which can reach more than 100 fold the
30 mean annual discharge (Delrieu et al. 2005; Dezileau et al. 2014). These floods are caused by

1 heavy rainfalls: precipitations greater than 200 mm can be recorded in a single day while the
2 average annual precipitation ranges between 500 and 1100 mm (Dezileau et al., 2014).

3 During the studied period, three main flood events occurred in March 2011, November
4 2011 and March 2013 (Figure 2a). The instantaneous peak discharge and average daily
5 discharge at Ners reached 716 m³/s and 403 m³/s, respectively, in March 2011, 1110 m³/s and
6 670 m³/s in November 2011, 820 m³/s and 431 m³/s in March 2013 (Banque Hydro website).

7 3. Materials and methods

8 3.1. Sampling

9 3.1.a. *Spatial sampling*

10 Three spatial sampling campaigns were carried out throughout the Upper Gardon River
11 watershed in 2011 and 2012; sample locations are indicated on Figure 1. One campaign in
12 December 2012 was representative of winter low flow conditions (no significant rainfall in
13 the previous 3 weeks). Campaigns in March 2011 and November 2011 were carried out
14 during high flow periods, one and four days after the flood peak of two major floods,
15 respectively (Figure 2).

16 For the three campaigns, water samples for the analysis of dissolved metal(loid)
17 concentrations were filtered in the field as described in section 3.2.a. In November 2011, SPM
18 and particulate metal(loid) concentrations were also determined. For this, 2 L of raw water
19 were sampled in acid-cleaned HDPE bottles and filtered immediately back to the laboratory as
20 described in section 3.2.b.

21 3.1.b. *Flood monitoring*

22 Two consecutive flood events (Event 1 on 6-7 March 2013 and Event 2 on 17-18 March
23 2013, Figure 2b) were monitored with high resolution sampling during 24 h each at two
24 sampling sites (1) at the station “Lezan” situated ~7 km upstream from the outlet of the
25 Gardon of Anduze subwatershed and (2) at the station “Ners” (station 10) downstream from
26 the confluence between the Gardon of Anduze and the Gardon of Ales Rivers (Figure 1).
27 Hourly discharge reached 171 m³/s at Anduze station (~6 km upstream from the Lezan site)
28 and 206 m³/s at Ners station during Event 1; it reached 527 m³/s and 811 m³/s, respectively,

1 during Event 2. This second flood event was characterized by a temporary steady flow pattern
2 during the rising limb of the hydrograph (Figure 2b).

3 Flood samples were collected using two automatic samplers manually triggered (Sigma
4 SD900 at the Lezan site and Isco 6712 at the Ners site). Water was pumped using a peristaltic
5 pump and a ~10 m PTFE sampling tube. Its outlet was equipped with a polypropylene strainer
6 and fixed on a bridge pier (Lezan station) or a water mill wall (Ners station) to prevent the
7 sampling tube washout during floods. In such a way, water was pumped at 1 m from the
8 riverbank and 0.5 m above the riverbed. Such a setting was shown to be adapted to automatic
9 sampling in river systems (Coynel et al., 2004).

10 Automatic samplers were scheduled to collect a sample of 1 L every hour during a 24 h-
11 period. An automatic purge allowed rinsing the sampling tube before each sampling to avoid
12 sample cross-contamination. Water samples were stored in acid-cleaned 1 L polypropylene
13 bottles. Finally, samples were retrieved at the end of the program (within 6 h) and were
14 filtered back to the laboratory within less than 72 hours after collection. For technical reasons,
15 the record of the Event 1 started at the flood peak at Lezan and 4h before the flood peak at
16 Ners.

17 3.2. Sample treatment

18 3.2.a. *Dissolved metal(loid) concentrations*

19 Filtrations were performed using a syringe and a disposable 0.22 μm cellulose acetate
20 syringe filter rinsed with river water before sample filtration. Filtrates were collected in acid-
21 cleaned HDPE bottles, acidified to 1% with HNO_3 (14.5 M, suprapur) and stored at 4 $^\circ\text{C}$ until
22 analysis. The filtrate will be referred to dissolved fraction, although colloidal particles may
23 pass through 0.22 μm filters.

24 3.2.b. *SPM concentrations*

25 Determination of SPM concentrations was performed by filtration of a precise volume
26 (from 150 mL to 900 mL) of homogenized water through acid-cleaned, dried and pre-weighed
27 0.22 μm PTFE filters (Millipore) fitted on polycarbonate filter holders (Sartorius). Then,
28 filters were dried in a desiccator until constant weight. Three successive weighing were
29 performed after the drying step to estimate weight reproducibility. The collected SPM mass
30 ranged from 4.7 mg to 194 mg (43 mg of average). Weighing error (relative standard

1 deviation) was better than 5% even for low masses. Filters were stored in a freezer for
2 subsequent acid digestion and particulate metal(loid) concentration determination.

3 *3.2.c. Particulate metal(loid) concentrations*

4 Filters with SPM were digested in closed Teflon reactors on hot-plates at 100°C for 24 h
5 with 4 mL HNO₃ (14.5 M, suprapur) and 3 mL HF (22.6 M, suprapur). After cooling, filters
6 were rinsed with double deionized water (Milli-Q) and removed. The remaining solutions
7 were evaporated to dryness at 65 °C. Finally, samples were brought to 30 mL using 3 mL
8 HNO₃ (14.5 M, suprapur) and 27 mL of double deionized water (Milli-Q). For each set of
9 samples, method blanks and certified reference river sediments (NCS DC70317 from LGC
10 Standards) were digested in the same way.

11 3.3. Analysis

12 *3.3.a. Determination of dissolved and particulate metal(loid) concentrations*

13 Dissolved and particulate metal (Cd, Pb, Tl, Zn) and metalloid (As, Sb) concentrations
14 were measured using ICP-MS (X7 Series II and iCAP Q, equipped with a CCT – Collision
15 Cell Technology chamber – Thermo Scientific). Concentrations were determined with
16 external calibration using In and Bi as internal standards to correct potential sensitivity drifts.
17 The quality of analysis was checked by analyzing international certified reference waters
18 (CNRC SLRS-5, NIST SRM 1643e). Accuracy was better than 5% relative to the certified
19 values and analytical error (relative standard deviation) was better than 5% for concentrations
20 ten times higher than the detection limits.

21 For mineralized solid samples, accuracy was within 10% of the certified values for
22 reference standards (NCS DC70317 from LGC Standards, n=5). Finally, mineralization
23 blanks represented less than 5 % of particulate metal(loid) concentrations; except for Sb and
24 Zn in a set of samples for which these elements were excluded from the results.

25 *3.3.b. Assessment of the potential alteration of samples during storage in automatic 26 sampler*

27 To evaluate potential sample alteration during storage in the automatic sampler (e.g.
28 eventual sorption of metal(loid) onto SPM or bottle walls), we compared dissolved

1 concentrations in two samples from stations Lezan and Ners after immediate filtration in the
2 field and after 72 h storage at 6-10 °C followed by filtration in the laboratory (Table 2).

3 Recovery averaged 100% for As, Cd and Sb in the dissolved fraction after 72 h storage
4 whatever the hydrological conditions (high or low SPM concentration). Conversely, recovery
5 was lower than 100% for Pb and Zn and higher than 100% for Tl, showing adsorption (Pb,
6 Zn) or desorption (Tl) of these elements onto/from SPM during 72h storage, in an extent
7 which appeared to depend on SPM concentration (Table 2). Therefore, temporal variations of
8 dissolved concentrations during the flood will be presented only for As, Cd and Sb.

9 However, particulate concentrations will be presented for all studied metals and
10 metalloids (As, Cd, Pb, Sb, Tl and Zn) because the contribution of adsorption (Pb, Zn) or
11 desorption (Tl) evidenced during storage (Table 2) and that modified significantly dissolved
12 concentration values for Pb, Zn and Tl appeared to affect very slightly particulate
13 concentrations. Indeed, concerning Tl in samples from the monitored flood, if we consider
14 that all Tl present in the dissolved phase originates from desorption during storage (which is
15 the worst case), particulate Tl concentrations during the flood would be underestimated by no
16 more than 26% (Supporting Information, Figure 1). Concerning Pb and Zn, previous
17 unpublished dissolved concentration data obtained after filtration in the field in various
18 hydrological conditions (high and low flow) at Lezan (n = 5) and Ners (n = 4) indicated low
19 values, less than 0.82 µg/L for Pb and less than 6.3 µg/L for Zn (Supporting Information,
20 Figure 2), showing that dissolved Pb and Zn concentrations were low whatever hydrological
21 conditions. Dissolved concentrations represented 18% (Zn) and 5% (Pb) of total (dissolved +
22 particulate) Zn and Pb concentrations in our November 2011 survey (section 4.1.b), in
23 agreement with the predominant association of these elements to the particulate phase in river
24 systems at near neutral pH (Gaillardet et al. 2003; Masson et al. 2006; Ollivier et al. 2011).
25 Thus, Pb and Zn present in the dissolved phase in our flood samples would reasonably not
26 contribute to increase significantly the particulate concentration values during storage.

27 *3.3.c. Metal(loid) load assessment*

28 Dissolved loads of As and Sb during the second monitored 24 h-flood at Ners were
29 calculated using hourly discharge (Q_h) (Banque Hydro website) and hourly dissolved
30 concentrations (C_d) (Equation 1). Particulate loads of metal(loid)s were estimated using
31 hourly discharge, hourly SPM concentration (C_{SPM}) and hourly particulate metal(loid)
32 concentrations (C_p) (Equation 2).

1 Dissolved load: $L_D = \sum(Q_h \times C_d)$ Eq. 1

2 Particulate load: $L_P = \sum(Q_h \times C_{SPM} \times C_p)$ Eq. 2

3 4. Results

4 4.1. Spatial distribution of dissolved and particulate metal(loid) concentrations
5 at high and low flow

6 4.1.a. *Dissolved metal and metalloid concentrations*

7 Dissolved concentrations of the studied elements along the Gardon River watershed
8 exceeded world river averages up to 3- (Pb), 13- (As), 19- (Zn), 52- (Tl) and 161-fold (Sb),
9 with the exception of Cd (Figure 3) (Gaillardet et al. 2003). The highest concentrations were
10 obtained at low flow for Cd, Sb, Tl and Zn (stations 4 and 5 for Cd, Tl and Zn; stations 2 to 5
11 for Sb, Figure 3) and at high flow for Pb (stations 2 to 4 and 8 to 10) while As concentration
12 did not vary significantly between high flow and low flow during these spatial surveys,
13 showing different dynamics of the studied elements relatively to hydrological conditions. The
14 concentrations of Cd, Sb, Tl and Zn were higher along the Gardon of Ales subwatershed
15 (Figure 3b, 3d, 3e, 3f, zone 1) than along the Gardon of Anduze subwatershed (Figure 3b, 3d,
16 3e, 3f, zone 2), while the reverse was observed for As (Figure 3a); no clear trend was
17 evidenced for Pb in the dissolved phase (Figure 3c). For Sb, a general decrease of dissolved
18 concentrations was observed from upstream to downstream stations along the Gardon of Ales
19 subwatershed (Figure 3d, zone 1). This dilution pattern suggests that the predominant Sb
20 sources were localized at the uppermost course of the subwatershed, where ancient Sb mines
21 are present. Conversely, Cd, Tl and Zn concentrations increased from upstream (1, 2, 3) to
22 downstream (4, 5) stations along the Gardon of Ales subwatershed, showing significant inputs
23 downstream station 3, where several Pb/Zn mines and the urban area of Ales are localized
24 (Figure 1).

25 Finally, dissolved concentrations downstream from the junction between the two
26 subwatersheds (station 10) clearly reflected the predominant flow contribution of the Gardon
27 of Anduze River upon the Gardon of Ales River (average discharge ratio 2:1, Banque Hydro
28 data), with As concentration at station 10 similar to station 9 while significant dilution was
29 evidenced for Cd, Sb, Tl and Zn from station 5 to station 10.

1 4.1.b. *Particulate metal and metalloid concentrations*

2 Particulate As, Cd, Pb, Sb, Tl and Zn concentrations in SPM recovered at high flow
3 exceeded world river averages up to 2 (As, Pb, Zn), 4 (Tl) and 25 fold (Sb) with the exception
4 of Cd (Figure 4).

5 The particulate phase represented on average 36% (Sb), 43% (As), 57% (Cd), 82% (Tl,
6 Zn) and 95% (Pb) of total (dissolved + particulate) concentrations, showing significant
7 contribution of particulate over dissolved load to metal transport during high (receding) flow.

8 Spatial distribution showed extremely higher concentrations of Sb in SPM along the
9 Gardon of Ales subwatershed compared to the Gardon of Anduze subwatershed (Figure 4d),
10 as already observed for dissolved Sb, and subsequent dilution in particles at the junction
11 between the two subwatersheds (station 10), confirming the predominance of Sb source on the
12 upper course of the Gardon of Ales subwatershed. For other metal(loid), particulate
13 concentrations did not show clear trend from upstream to downstream stations in both
14 subwatersheds indicating that there were more than one predominant source for these
15 metal(loid)s.

16 4.2. Flood monitoring

17 4.2.a. *Dissolved As, Cd and Sb concentrations*

18 The pattern of dissolved As concentrations during the two consecutive flood events
19 (Figure 5a, 5d) differed from that of Sb (Figure 5b, 5e) and Cd (Figure 5c, 5f). Arsenic
20 concentration increased with the discharge during Event 2, with a few hours shift between the
21 two consecutive upstream (Lezan) and downstream (Ners) stations (Figures 5a, 5d).
22 Concentration reached 10.2 µg/L at Lezan (17/03/2013 at 06:00) and 7.3 µg/L at Ners
23 (17/03/2013 at 09:00), which exceeded the values obtained during the winter low flow
24 conditions. This first peak coincided with a stationary flow phase occurring during the rising
25 limb of the hydrograph (Event 2', Figure 5a, 5d) in response to a temporary rainfall decrease
26 (data not shown). A second peak occurred (Event 2'', Figure 5a, d), with As concentration
27 reaching 5.7 µg/L, both at Lezan (17/03/2013 at 16:00) and Ners (17/03/2013 at 17:00). A
28 concentration peak was also visible during Event 1 at Ners (Figure 5d) but it was missed at
29 Lezan (Figure 5a), due to the time shift. Conversely, Sb concentration decreased with
30 increasing discharge during Event 2 at Ners (Figure 5e) and increased at receding flow during

1 Event 1, ranging between the high and low flow values recorded at this station (10) during the
2 spatial surveys. At Lezan, dissolved Sb concentration remained low and relatively stable
3 during the flood (Figure 5b), with a value of 0.17 ± 0.01 $\mu\text{g/L}$ which is lower than the
4 concentration measured during winter low flow. For Cd, dissolved concentrations also
5 decreased with increasing discharge during Event 2 at Lezan and during Event 1 at Ners. At
6 Lezan, the concentrations recorded during the flood were higher than the winter low flow
7 values, indicating that a concentration peak was probably missed at the early stage of the
8 floods while at the Ners station, Cd presented a dilution pattern compared to winter low flow
9 level (Figure 5c, 5f).

10 *4.2.b. SPM and particulate metal and metalloid concentrations*

11 SPM concentration increased with the discharge during Events 1 and 2; it reached
12 higher values during Event 2 (334 mg/L at Lezan and 647 mg/L at Ners) than during Event 1
13 (73 mg/L at Lezan and 141 mg/L at Ners), in relation with a higher discharge (Figure 6).
14 During Event 2, a first SPM peak coincided with the stationary flow phase occurring during
15 the rising limb of the hydrograph (Figure 6).

16 The pattern of particulate metal(loid) concentrations during the floods was similar to
17 that of dissolved As concentrations; two consecutive peaks were recorded during the rising
18 limb of Event 2 for As, Cd, Pb, Sb, Tl and Zn at Lezan (Figure 7a,7b) and for As, Pb and Zn
19 at Ners (Figure 7c), with lower concentration values at downstream station Ners located at the
20 junction between the two subwatersheds compared to upstream station Lezan, located at the
21 lowermost course of the Gardon of Anduze River. These concentrations during flood event 2
22 were higher than those recorded at high (receding) flow during the spatial survey, by a factor
23 1 to 3 for Sb, 2 to 6 for Zn and Tl, 2 to 11 for Pb, 3 to 14 for Cd, and 5 to 20 for As. This may
24 suggest the contribution of a common source highly enriched with these metal(loid)s in the
25 particulate phase during flood event 2 on the Gardon of Anduze subwatershed.

26 By plotting Pb versus As and Tl versus Cd concentration data from Event 2 at Lezan, a
27 distribution along two different correlation lines was observed, corresponding to Event 2' and
28 2'' (Figure 8a, 8b). SPM from Event 2' were more enriched with As and Cd compared to SPM
29 from Event 2'' which were more enriched with Pb and Tl. Correlation line from Event 2' fitted
30 with Pb-As data from Amous River SPM and surface bed deposit (Figure 8c); this river is
31 located downstream from the Carnoulès Pb-Zn mine, where exceptionally high As

1 concentrations were recorded in the drainage waters and associated secondary precipitates
2 (Leblanc et al. 1996; Casiot et al. 2003, 2009; Héry et al. 2014). Correlation line from Event
3 2” fitted both with Pb-As and Tl-Cd Amous River bulk sediment data and also with the Ourne
4 and Aiguesmortes Rivers sediment data (Figure 8c, 8d); these two latest rivers are located
5 downstream from the ancient mining district of Pallières which is close to Carnoulès mining
6 district. Correlation line from Event 2” also fitted with data from sulfide-rich tailings of the
7 Carnoulès mine and with data from a sediment layer in a flooding terrace recovered at 45 km
8 downstream from Lezan; this contaminated layer was attributed to the failure of a tailing dam
9 at the Carnoulès mine (Dezileau et al. 2014; Resongles et al. 2014).

10 5. Discussion

11 The Gardon River is a typical Mediterranean mid-size river that has been durably
12 impacted by metal contamination from ancient mining activity (Resongles et al. 2014). Levels
13 of As, Pb, Sb, Tl and Zn in the dissolved and particulate phases recorded in the present study
14 showed enrichments relatively to average river values, in agreement with the contamination
15 status of sediments and the high geochemical background established in a previous study
16 (Resongles et al. 2014). For As, Cd, Pb, Tl and Zn, the dissolved and particulate concentration
17 values were within the range of other mid-size rivers impacted by ancient mines (Table 3).
18 For Sb, the present data showed higher values than those recorded for the Isle and Lot Rivers
19 impacted by ancient mines from the western border of the French Massif Central (Coyne et
20 al. 2007; Grosbois et al. 2009).

21 The spatial distribution of metal(loid) contamination in the dissolved and particulate
22 phases corroborated previous sediment characterization along the Gardon River watershed
23 (Resongles et al. 2014). In this previous study, Cd, Sb, and Zn appeared to be enriched in the
24 sediments along the Gardon of Ales subwatershed relatively to the Gardon of Anduze
25 subwatershed, with predominant sources localized at the uppermost course of the river (Sb)
26 and around Ales urban and Pb/Zn mining area (Cd, Zn). For other elements (As, Pb, Tl), the
27 concentrations in the sediments upstream from the junction between the two subwatersheds
28 was similar (Resongles et al. 2014), these elements being associated to ancient Pb/Zn mines
29 present on both subwatersheds.

30 In the present study, the level of contamination and the contribution of the different
31 sources were shown to vary with hydrological conditions. For Sb, a decrease of dissolved

1 concentrations was observed at high flow on the Gardon of Ales subwatershed compared to
2 low flow conditions and a dilution pattern was also evidenced after the junction between the
3 two subwatersheds during the flood events. This was attributed to a dilution effect generally
4 observed with increasing river discharge (Grimshaw et al. 1976; Cánovas et al. 2008, 2012;
5 Grosbois et al. 2009; Ollivier et al. 2011). For As, dissolved concentrations along the Gardon
6 of Anduze River were similar at low and high (receding) flow. Nevertheless, these relatively
7 stable dissolved As levels have been exceeded two-fold during flood event 2 at Lezan,
8 showing that unusual As levels may be reached during such peculiar hydrological events.
9 Indeed, surface leaching processes occurring during rising floods may upgrade the usual As
10 levels; these processes involve flushing of surface tailings and contaminated soils, desorption
11 from As-rich particles from riverbed in mine-impacted tributaries; such flushing events were
12 often observed during floods in mining areas (Grimshaw et al. 1976; Cánovas et al. 2008;
13 Byrne et al. 2013). As an example, Masson et al. (2007) observed maximum dissolved As
14 concentrations in the Garonne River during a major flood event due to heavy rainfalls in the
15 upper Lot River watershed which is known for important potential As point sources such as
16 mining wastes, tailings and contaminated reservoir sediments. The concentration of the other
17 studied elements (Cd, Pb, Zn, Tl) in the particulate phase was also significantly increased
18 during flood event 2 at Lezan and also at Ners, relatively to receding flow of November 2011,
19 making the Gardon of Anduze subwatershed the predominant contributor to downstream
20 particulate As, Pb, Zn, Cd and Tl load during this peculiar flood event. Increasing metal(loid)
21 concentration in SPM during floods can be due to several processes such as remobilization of
22 contaminated sediments from the riverbed or the riverbank and erosion of soil and waste
23 deposits at mining sites caused by surface runoff. Here, the two successive contamination
24 peaks and associated distinct Pb-As and Tl-Cd correlations evidenced during the rising flood
25 of Event 2 at Lezan clearly highlighted that two different predominant sources or transport
26 mechanisms were involved during this flood. The mobilization of particles highly enriched
27 with As and Cd and in a lesser extent with Pb (Event 2') was followed by the mobilization of
28 particles highly enriched with Pb and Tl and in a lesser extent with As and Cd (Event 2''). The
29 corresponding activated sources or mechanisms are difficult to discriminate since floods are
30 complex events. Source contribution depends on the spatial and temporal repartition of
31 rainfalls and the distance between the source and the sampling station (Coynel et al. 2007). In
32 the present study, the main potential sources of As and Pb on the Gardon of Anduze
33 subwatershed are the mining districts of Carnoulès and Pallières (Figure 1, Table 1). During
34 Event 2, these mining districts were roughly equally affected by rainfalls; they recorded about

1 140 mm of precipitations in 36 hours (data from Meteo-France). Moreover, the two mines are
2 nearly equidistant from the flood monitoring station of Lezan, thus both mining sites may
3 have contributed to increase metal(loid) levels in SPM during flood event 2. Thus, the two
4 correlation lines may rather reflect the composition of different kinds of particles, being more
5 or less easily flushed as the flow rate increased. SPM of Event 2' exhibited Pb/As and Tl/Cd
6 ratios of 0.5 and 0.7 and the corresponding correlation line fitted with some of the Amous
7 River SPM highly enriched with arsenic (Pb/As and Tl/Cd ratios of 0.5 and 0.2 on average,
8 Figure 8c). This correlation also fitted with few data from fine Fe-rich superficial Amous
9 River bed deposits (Pb/As and Tl/Cd ratios of 0.3 and 0.04 on average); these deposits were
10 orange loosely packed and watery, they were deposited onto the top of Amous river bed (Héry
11 et al. 2014). Their consistency makes these deposits prone to flushing as soon as the flow rate
12 increases. SPM corresponding to Event 2'' presented higher Pb/As and Tl/Cd ratios of 2.3 and
13 2.5 and the correlation line fitted with data from sulfide-rich tailings from the Carnoulès mine
14 (Pb/As and Tl/Cd ratios of 3.6 and 4.5 on average), also with sediment data from rivers
15 draining the ancient mining districts of Carnoulès and Pallières (Pb/As and Tl/Cd ratios of 6.4
16 and 1.5 on average, Figure 8c, 8d) (Resongles et al. 2014). Moreover, this correlation line also
17 fitted with data from a sedimentary archive layer located at a downstream station in the
18 Gardon River; this layer corresponded to sulfide-rich sands originating from the failure of a
19 tailings dam at Carnoulès in 1976 (Pb/As and Tl/Cd ratios of 2.8 on average). Therefore, the
20 geochemical signature of SPM transported during Event 2' may be related to the
21 remobilization of easily flushed secondary precipitates temporarily stored in the streambed in
22 the vicinity of Carnoulès mine while SPM transported during Event 2'' may reflect the
23 contribution of primary sulfides originating from tailings or from downstream diffuse sources
24 (remobilization of these primary sulfides stored temporarily in riverbed or riverbank) which
25 may have a similar composition in As, Pb, Tl and Cd throughout the whole Carnoulès-
26 Pallières mining area. Such sulfide-rich grey sands were observed after storm events at the
27 outlet of the drain that crossed the tailings pile at Carnoulès and in the streambed of the small
28 Reigous Creek that flows into the Amous River.

29 Altogether, these results highlight the importance of flood events in the mobilization of
30 metal(loid)s in the Gardon River. Exceptionally high particulate concentrations of As were
31 reached during flood event 2 in the present study, compared to other mining-impacted rivers;
32 the values reached 1233 mg/kg at Lezan and greatly exceeded European guidelines for
33 sediment quality (Macklin et al. 2006). Considering the dissolved and particulate loads

1 downstream from the junction between the two subwatersheds (Ners station), our calculations
2 indicated dissolved As, Cd and Sb loads reaching 204 kg, 0.5 kg and 19.4 kg, respectively and
3 particulate load reaching 1915 kg for As, 24 kg for Cd, 94 kg for Sb, 38 kg for Tl, 2860 kg for
4 Pb and 5214 kg for Zn within 24 h during Event 2. Although these particulate metal(loid)
5 loads are significant, they are relatively low compared to those exported from the Lot River
6 watershed that also drained ancient mines from the western border of the French Massif
7 Central, besides receiving inputs from an ancient Zn smelter. The particulate load of the Lot
8 River during a 5-days major flood was about 14 times (As), 18 times (Pb), 47 times (Sb), 164
9 times (Zn) and 349 times (Cd) higher than the particulate load of the Gardon River during the
10 flood Event 2, in relation with a 30 times higher SPM load (Coynel et al. 2007) and a higher
11 level of Cd and Zn (Table 3).

12 The geochemical signature of the Gardon River, characterized by relatively high
13 dissolved As and Sb concentrations, was evidenced during three important flood events
14 recorded on the Rhône River in 2002 and 2003 (Ollivier et al. 2006). During these floods,
15 dissolved As (1-5 µg/L) and Sb (0.2-0.7 µg/L) concentrations in the Rhône River at Arles,
16 downstream from the junction with the Gardon River, were close to those recorded in the
17 present study (3-7 µg/L for As and 0.3-0.9 µg/L for Sb) during the floods at Ners; this was
18 related to the unusual contribution of Cevenol tributaries to the whole Rhône flow during the
19 2002 and 2003 flood events. In particular, Cevenol tributaries accounted for 90% of the
20 Rhône flow at Arles during the September 2002 flood event (Ollivier et al. 2006, 2011).

21 6. Conclusion

22 In this study, high-temporal flood monitoring allowed to evidence that significant
23 temporal variations of dissolved and particulate metal (Cd, Pb, Tl, Zn) and metalloid (As, Sb)
24 concentrations occurred during Mediterranean flood in the former mining watershed of the
25 Gardon River. Dissolved Sb concentration was affected by usual dilution processes often
26 observed with increasing discharge. Conversely, dissolved As and particulate As, Cd, Pb, Tl
27 and Zn concentrations exhibited two successive contamination peaks during the rising flood
28 with higher concentrations than those recorded during low or receding flow conditions
29 showing that mine-related sources were activated during the flood.

30 The correlation between particulate As, Pb, Tl and Cd concentrations showed two
31 different signatures associated with the two contamination peaks, suggesting that two

1 different kinds of contaminated particles were successively transported during the studied
2 flood in the Gardon River system. Based on the location of the potential contamination
3 sources and the geochemical signature of associated contaminated particles, we could infer
4 that the first group of particles might be ascribed to the flushing of secondary precipitates
5 which are commonly found in mining streams affected by acid mine drainage. The second
6 group might correspond to primary sulfides originating from tailings or from downstream
7 secondary sources. However, further work is necessary to distinguish between point sources
8 and diffuse downstream sources of such particles.

9 Finally, this study highlighted the importance of floods in the mobilization of metals
10 and metalloids from ancient mining sites in Mediterranean regions, showing the need for
11 monitoring flood events to understand metal and metalloid transport in such river systems and
12 accurately assess the long-term contribution of mining activity to metal(loid) loads of
13 downstream watershed. Further research is needed to estimate the contribution of this kind of
14 flood event to annual metal(loid) flux.

1 Acknowledgments

2 The authors would like to thank Pierre Marchand, Maurice Guilliot and Frédéric Hernandez
3 for field assistance and Sophie Delpoux for laboratory analysis. Valérie Borrell is thanked for
4 fruitful discussions. The municipality of Boucoiran is thanked for providing access to the mill
5 at Pont de Ners for automatic sampler installation. This study was supported by the EC2CO-
6 INSU program and OSU OREME (<http://www.oreme.univ-montp2.fr>).

7 References

- 8 Alkaaby, A., 1986. Conglomérats minéralisés (Pb-Ba-Fe) du Trias basal sur la bordure sud-est des Cévennes :
9 exemple du système fluvial en tresse de Carnoulès (Gard). Thesis Université des Sciences et Techniques
10 du Languedoc, p.154.
- 11 Audry, S., 2003. Bilan géochimique du transport des éléments traces métalliques dans le système fluvial
12 anthropisé Lot-Garonne-Gironde. Thesis Université de Bordeaux I, p.413.
- 13 Axtmann, E., Luoma, S., 1991. Large-scale distribution of metal contamination in the fine-grained sediments of
14 the Clark Fork River, Montana, U.S.A. *Applied Geochemistry* 6, 75–88.
- 15 Banque Hydro, Eaufrance. Last accessed on 30/08/2014, <http://www.hydro.eaufrance.fr/>.
- 16 Bradley, S., Lewin, J., 1982. Transport of heavy metals on suspended sediments under high flow conditions in a
17 mineralised region of Wales. *Environmental Pollution* 4, 257–267.
- 18 Bradley, S.B., 1984. Flood effects on the transport of heavy metals. *International Journal of Environmental*
19 *Studies* 22, 225–230.
- 20 BRGM, ADES. Portail National d'Accès aux Données sur les Eaux Souterraines Last accessed on 30/08/2014,
21 <http://www.ades.eaufrance.fr/>.
- 22 BRGM, InfoTerre. Last accessed on 30/08/2014, <http://infoterre.brgm.fr/>.
- 23 BRGM, SIG Mines. Last accessed on 30/08/2014, <http://sigminesfrancebrgmfr/>.
- 24 Byrne, P., Wood, P.J., Reid, I., 2012. The Impairment of River Systems by Metal Mine Contamination: A
25 Review Including Remediation Options. *Critical Reviews in Environmental Science and Technology* 42,
26 2017–2077.
- 27 Byrne, P., Reid, I., Wood, P.J., 2013. Stormflow hydrochemistry of a river draining an abandoned metal mine:
28 the Afon Twymyn, central Wales. *Environmental Monitoring and Assessment* 185, 2817–32.
- 29 Cánovas, C.R., Hubbard, C.G., Olías, M., Nieto, J.M., Black, S., Coleman, M.L., 2008. Hydrochemical
30 variations and contaminant load in the Río Tinto (Spain) during flood events. *Journal of Hydrology* 350,
31 25–40.
- 32 Cánovas, C.R., Olías, M., Sarmiento, A.M., Nieto, J.M., Galván, L., 2012. Pollutant transport processes in the
33 Odiel River (SW Spain) during rain events. *Water Resources Research* 48, W06508.
- 34 Cánovas, C.R., Olías, M., Nieto, J.M., Galván, L., 2010. Wash-out processes of evaporitic sulfate salts in the
35 Tinto River: Hydrogeochemical evolution and environmental impact. *Applied Geochemistry* 25, 288–301.
- 36 Casiot, C., Leblanc, M., Bruneel, O., Personné, J.-C., Koffi, K., Elbaz-Poulichet, F., 2003. Geochemical
37 Processes Controlling the Formation of As-Rich Waters Within a Tailings Impoundment (Carnoulès,
38 France). *Aquatic Geochemistry* 9, 273–290.
- 39 Casiot, C., Egal, M., Elbaz-Poulichet, F., Bruneel, O., Bancon-Montigny, C., Cordier, M.-A., Gomez, E.,
40 Aliaume, C., 2009. Hydrological and geochemical control of metals and arsenic in a Mediterranean river
41 contaminated by acid mine drainage (the Amous River, France); preliminary assessment of impacts on fish
42 (*Leuciscus cephalus*). *Applied Geochemistry* 24, 787–799.

- 1 Coulthard, T.J., Macklin, M.G., 2003. Modeling long-term contamination in river systems from historical metal
2 mining. *Geology* 31, 451-454.
- 3 Coynel, A., Schäfer, J., Hurtrez, J.-E., Dumas, J., Etcheber, H., Blanc, G., 2004. Sampling frequency and
4 accuracy of SPM flux estimates in two contrasted drainage basins. *Science of the Total Environment* 330,
5 233-247.
- 6 Coynel, A., Schäfer, J., Blanc, G., Bossy, C., 2007. Scenario of particulate trace metal and metalloid transport
7 during a major flood event inferred from transient geochemical signals. *Applied Geochemistry* 22, 821-
8 836.
- 9 David, A., Bancon-Montigny, C., Salles, C., Rodier, C., Tournoud, M.-G., 2012. Contamination of riverbed
10 sediments by hazardous substances in the Mediterranean context: Influence of hydrological conditions.
11 *Journal of Hydrology* 468-469, 76-84.
- 12 Dawson, E.J., Macklin, M.G., 1998. Speciation of heavy metals on suspended sediment under high flow
13 conditions in the River Aire, West Yorkshire, UK. *Hydrological Processes* 12, 1483-1494.
- 14 Delrieu, G., Ducrocq, V., Gaume, E., Nicol, J., Payrastra, O., Yates, E., Kirstetter, P., Andrieu, H., Ayral, P.,
15 Bouvier, C., Creutin, J., Livet, M., Anquetin, S., Lang, M., Neppel, L., Obled, C., Parent-Du-Chatelet, J.,
16 Saulier, G., Walpersdorf, A., Wobrock, W., 2005. The catastrophic flash-flood event of 8-9 September
17 2002 in the Gard region, France: a first case study for the Cévennes-Vivarais Mediterranean
18 Hydrometeorological. *Journal of Hydrometeorology* 6, 34-52.
- 19 Dennis, I.A., Macklin, M.G., Coulthard, T.J., Brewer, P.A., 2003. The impact of the October-November 2000
20 floods on contaminant metal dispersal in the River Swale catchment, North Yorkshire, UK. *Hydrological*
21 *Processes* 17, 1641-1657.
- 22 Dezileau, L., Terrier, B., Berger, J.F., Blanchemanche, P., Latapie, A., Freydier, R., Bremond, L., Paquier, A.,
23 Lang, M., Delgado, J.L., 2014. A multidating approach applied to historical slackwater flood deposits of
24 the Gardon River, SE France. *Geomorphology* 214, 56-68.
- 25 Foulds, S.A., Brewer, P.A., Macklin, M.G., Haresign, W., Betson, R.E., Rassner, S.M.E., 2014. Flood-related
26 contamination in catchments affected by historical metal mining: An unexpected and emerging hazard of
27 climate change. *Science of the Total Environment* 476-477, 165-180.
- 28 Gaillardet, J., Viers, J., Dupré, B., 2003. Trace elements in river waters. *Treatise on Geochemistry* 5, 225-272.
- 29 Gao, Y., Bradshaw, A.D., 1995. The containment of toxic wastes: II. Metal movement in leachate and drainage
30 at Parc lead-zinc mine, North Wales. *Environmental Pollution* 90, 379-382.
- 31 Gozzard, E., Mayes, W.M., Potter, H.A.B., Jarvis, A.P., 2011. Seasonal and spatial variation of diffuse (non-
32 point) source zinc pollution in a historically metal mined river catchment, UK. *Environmental Pollution*
33 159, 3113-3122.
- 34 Gray, N.F., 1998. Acid mine drainage composition and the implications for its impact on lotic systems. *Water*
35 *Research* 32, 2122-2134.
- 36 Grimshaw, D., Lewin, J., Fuge, R., 1976. Seasonal and short-term variations in the concentration and supply of
37 dissolved zinc to polluted aquatic environments. *Environmental Pollution* 11, 1-7.
- 38 Grosbois, C., Schäfer, J., Bril, H., Blanc, G., Bossy, A., 2009. Deconvolution of trace element (As, Cr, Mo, Th,
39 U) sources and pathways to surface waters of a gold mining-influenced watershed. *Science of the Total*
40 *Environment* 407, 2063-2076.
- 41 Helios Rybicka, E., Adamiec, E., Aleksander-Kwaterczak, U., 2005. Distribution of trace metals in the Odra
42 River system: Water-suspended matter-sediments. *Limnologica* 35, 185-198.
- 43 Héry, M., Casiot, C., Resongles, E., Gallice, Z., Bruneel, O., Desoeuvre, A., Delpoux, S., 2014. Release of
44 arsenite, arsenate and methyl-arsenic species from streambed sediment impacted by acid mine drainage: a
45 microcosm study. *Environmental Chemistry*. <http://dx.doi.org/10.1071/EN13225>
- 46 Hudson-Edwards, K.A., 2003. Sources, mineralogy, chemistry and fate of heavy metal-bearing particles in
47 mining-affected river systems. *Mineralogical Magazine* 67, 205-217.

- 1 Hudson-Edwards, K.A., Schell, C., Macklin, M.G., 1999. Mineralogy and geochemistry of alluvium
2 contaminated by metal mining in the Rio Tinto area, southwest Spain. *Applied Geochemistry* 14, 1015–
3 1030.
- 4 Keith, D.C., Runnells, D.D., Esposito, K.J., Chermak, J.A., Levy, D.B., Hannula, S.R., Watts, M., Hall, L., 2001.
5 Geochemical models of the impact of acidic groundwater and evaporative sulfate salts on Boulder Creek at
6 Iron Mountain, California. *Applied Geochemistry* 16, 947–961.
- 7 Laslett, R., 1995. Concentrations of dissolved and suspended particulate Cd, Cu, Mn, Ni, Pb and Zn in surface
8 waters around the coasts of England and Wales and in adjacent seas. *Estuarine, Coastal and Shelf Science*
9 40, 67–85.
- 10 Leblanc, M., Achard, B., Othman, D. Ben, Luck, J., 1996. Accumulation of arsenic from acidic mine waters by
11 ferruginous bacterial accretions (stromatolites). *Applied Geochemistry* 11, 541–554.
- 12 Lehmann, J., Puff, T., Damke, H., Eidam, J., Henning, K.-H., Jülich, W.-D., Roßberg, H., 1999. The Odra river
13 load of heavy metals at Hohenwutzen during the flood in 1997. *Acta Hydrochimica Hydrobiologica* 27,
14 321–324.
- 15 MacKenzie, A., Pulford, I., 2002. Investigation of contaminant metal dispersal from a disused mine site at
16 Tyndrum, Scotland, using concentration gradients and stable Pb isotope ratios. *Applied Geochemistry* 17,
17 1093–1103.
- 18 Macklin, M.G., Brewer, P.A., Hudson-Edwards, K.A., Bird, G., Coulthard, T.J., Dennis, I.A., Lechler, P.J.,
19 Miller, J.R., Turner, J.N., 2006. A geomorphological approach to the management of rivers contaminated
20 by metal mining. *Geomorphology* 79, 423–447.
- 21 Macklin, M.G., Hudson-Edwards, K.A., Dawson, E.J., 1997. The significance of pollution from historic metal
22 mining in the Pennine orefields on river sediment contaminant fluxes to the North Sea. *Science of the*
23 *Total Environment* 194-195, 391–397.
- 24 Macklin, M.G., Klimek, K., 1992. Dispersal, storage and transformation of metal- contaminated alluvium in the
25 upper Vistula basin, southwest Poland. *Applied Geography* 12, 7–30.
- 26 Masson, M., Blanc, G., Schäfer, J., 2006. Geochemical signals and source contributions to heavy metal (Cd, Zn,
27 Pb, Cu) fluxes into the Gironde Estuary via its major tributaries. *Science of the Total Environment* 370,
28 133–146.
- 29 Masson, M., Schäfer, J., Blanc, G., Pierre, A., 2007. Seasonal variations and annual fluxes of arsenic in the
30 Garonne, Dordogne and Isle Rivers, France. *Science of the Total Environment* 373, 196–207.
- 31 Mayes, W.M., Johnston, D., Potter, H.A.B., Jarvis, A.P., 2009. A national strategy for identification,
32 prioritisation and management of pollution from abandoned non-coal mine sites in England and Wales. I.
33 Methodology development and initial results. *Science of the Total Environment* 407, 5435–5447.
- 34 Meybeck, M., 2001. Transport et qualité des sédiments fluviaux : de la variabilité spatio-temporelle à la gestion.
35 *La Houille Blanche* 34–43.
- 36 Mighanetara, K., Braungardt, C.B., Rieuwerts, J.S., Azizi, F., 2009. Contaminant fluxes from point and diffuse
37 sources from abandoned mines in the River Tamar catchment, UK. *Journal of Geochemical Exploration*
38 100, 116–124.
- 39 Miller, J., Barr, R., Grow, D., Lechler, P., Richardson, D., Waltman, K., Warwick, J., 1999. Effects of the 1997
40 Flood on the Transport and Storage of Sediment and Mercury within the Carson River Valley, West-
41 Central Nevada. *The Journal of Geology* 107, 313–327.
- 42 Miller, J.R., Hudson-Edwards, K.A., Lechler, P.J., Preston, D., Macklin, M.G., 2004. Heavy metal
43 contamination of water, soil and produce within riverine communities of the Río Pilcomayo basin, Bolivia.
44 *Science of the Total Environment* 320, 189–209.
- 45 Miller, J.R., Lechler, P.J., Mackin, G., Germanoski, D., Villarroel, L.F., 2007. Evaluation of particle dispersal
46 from mining and milling operations using lead isotopic fingerprinting techniques, Rio Pilcomayo Basin,
47 Bolivia. *Science of the Total Environment* 384, 355–373.
- 48 Moore, J., Luoma, S., 1990. Hazardous wastes from large-scale metal extraction. A case study. *Environmental*
49 *Science & Technology* 24, 1278–1285.

- 1 Ollivier, P., Radakovitch, O., Hamelin, B., 2006. Unusual variations of dissolved As, Sb and Ni in the Rhône
2 River during flood events. *Journal of Geochemical Exploration* 88, 394–398.
- 3 Ollivier, P., Radakovitch, O., Hamelin, B., 2011. Major and trace element partition and fluxes in the Rhône
4 River. *Chemical Geology* 285, 15–31.
- 5 Pont, D., Simonnet, J.-P., Walter, A.V., 2002. Medium-term Changes in Suspended Sediment Delivery to the
6 Ocean: Consequences of Catchment Heterogeneity and River Management (Rhône River, France).
7 *Estuarine, Coastal and Shelf Science* 54, 1–18.
- 8 Resongles, E., Casiot, C., Freydier, R., Dezileau, L., Viers, J., Elbaz-Poulichet, F., 2014. Persisting impact of
9 historical mining activity to metal (Pb, Zn, Cd, Tl, Hg) and metalloid (As, Sb) enrichment in sediments of
10 the Gardon River, Southern France. *Science of the Total Environment* 481, 509–521.
- 11 Schäfer, J., Blanc, G., 2002. Relationship between ore deposits in river catchments and geochemistry of
12 suspended particulate matter from six rivers in southwest France. *Science of the Total Environment* 298,
13 103–118.
- 14 SMAGE des Gardons, 2011. Etude de la qualité des eaux du bassin des Gardons. Phase 1 : Diagnostic, p.380.
- 15 Viers, J., Dupré, B., Gaillardet, J., 2009. Chemical composition of suspended sediments in World Rivers: New
16 insights from a new database. *Science of the Total Environment* 407, 853–868.
- 17 Young, P.L., 1997. The longevity of minewater pollution: a basis for decision-making. *Science of the Total*
18 *Environment* 194, 457–466.
- 19 Younger, P., Wolkersdorfer, C., 2004. Mining impacts on the fresh water environment: technical and managerial
20 guidelines for catchment scale management. *Mine Water and the Environment* 23, 2–80.
- 21 Žák, K., Rohovec, J., Navrátil, T., 2009. Fluxes of Heavy Metals from a Highly Polluted Watershed During
22 Flood Events: A Case Study of the Litavka River, Czech Republic. *Water, Air, and Soil Pollution* 203,
23 343–358.

1 Figure captions

2 Figure 1: Map of the studied area, showing the sampling station locations (details are given in Table 1 for
3 mining districts indicated by a letter A-F).

4 Figure 2: a) Daily discharge (in m³/s) measured at Ners from 2011 to 2013; arrows represent spatial
5 sampling campaign dates b) Hourly discharge in m³/s measured at Ners and at Anduze and Ales towns
6 during the two monitored floods of March 2013, crosses represent sample collection.

7 Figure 3: Spatial evolution of dissolved As, Cd, Pb, Sb, Tl and Zn concentrations from upstream to
8 downstream sites along the Gardon Ales River (zone 1), the Gardon Anduze River (zone 2) and
9 downstream from the confluence of these two rivers, at the Ners site (zone 3) under low flow and high flow
10 conditions. World river average values of dissolved concentrations from Gaillardet et al. (2003).

11 Figure 4: Spatial evolution of particulate As, Cd, Pb, Sb, Tl and Zn concentrations from upstream to
12 downstream sites along the Gardon Ales River (zone 1), the Gardon Anduze River (zone 2) and
13 downstream from the confluence of these two rivers, at the Ners site (zone 3) in SPM recovered during
14 high flow in November 2011. World river average values in SPM from Viers et al. (2009).

15 Figure 5: Temporal variations of dissolved As, Cd and Sb concentrations (in µg/L) and hourly discharge (in
16 m³/s) at Lezan (discharge measured at Anduze ~6 km upstream from Lezan site) and Ners during the
17 monitored floods of March 2013. The first point represents the dissolved concentrations measured during
18 winter low flow in December 2012. Horizontal dashed lines represent the concentration measured at station
19 8 (a, b and c) and station 10 (d, e, f) during the receding flow of November 2011.

20 Figure 6: Temporal variations of suspended particulate matter (SPM) concentration (in mg/L) and hourly
21 discharge (in m³/s) at Lezan (discharge measured at Anduze ~6 km upstream from Lezan site) and at Ners.

22 Figure 7: Temporal variations of particulate metal (Cd, Pb, Tl, Zn) and metalloid (As, Sb) concentrations
23 (in mg/kg) and hourly discharge (in m³/s) at Lezan (discharge measured at Anduze ~6 km upstream from
24 Lezan site) and Ners during the monitored floods of March 2013. Horizontal dashed lines represent the
25 concentration measured at station 8 (a, b) and station 10 (c, d) during the receding flow of November 2011.

26 Figure 8 : Relationship between a) Pb and As concentrations and b) Tl and Cd concentrations in SPM
27 collected during the flood Event 2 at Lezan. The geochemical background value of the Gardon River
28 watershed and sediments from flooding layers dated at 1976 are also shown. Relationship between c) Pb
29 and As concentrations and d) Tl and Cd concentrations in various contaminated materials collected on the
30 two main mining districts of the Gardon of Anduze River subwatershed (Carnoulès and Pallières mining
31 districts, Figure 1 and Table 1). The lines in panels c) and d) are extrapolations of regression lines shown in
32 panels a) and b).

33 *Concentrations are divided by 2 to fit into the scale

34 References : ¹this study, ²Resongles et al. 2014, ³unpublished data, ⁴Leblanc et al. 1996 (graph c only),
35 ⁵Casiot et al. 2009, ⁶Héry et al. 2014

36 Table captions

37 Table 1: Largest mining districts, their metal production, remaining wastes and the rivers that drain sites
38 (Alkaaby, 1986; BRGM, SIG Mines website).

39 Table 2 : Comparison of dissolved concentrations in the filtrates when filtration was performed at t=0 h and
40 t=72 h.

1 Table 3 : Dissolved and particulate metal(loid) concentrations from several European mining-impacted
2 rivers.

Mining district	Metal production	Mining wastes	Impacted river	Location code (Figure 1)
Carnoulès	Pb 30 000-65 000 t ; Zn 3500 t; Ag 20 t	1.3 Mt	Amous	A
Pallières	Zn 80 000 t; Pb 20 000 t; Ag 22 t	0.27 Mt	Ourne and Aiguesmortes	B
La Felgerette	Sb 2750 t	38 000 t	Ravin des Bernes	C
Le Soulier	Pyrite 4 Mt, Pb, Zn	1 Mt	Gardon of Ales, Grabieux	D
Rousson	Zn 4300 t, pyrite	n.d.	Avène	E
Saint Jean du Pin	Zn 1000 t; pyrite 2000 t	n.d.	Alzon	F

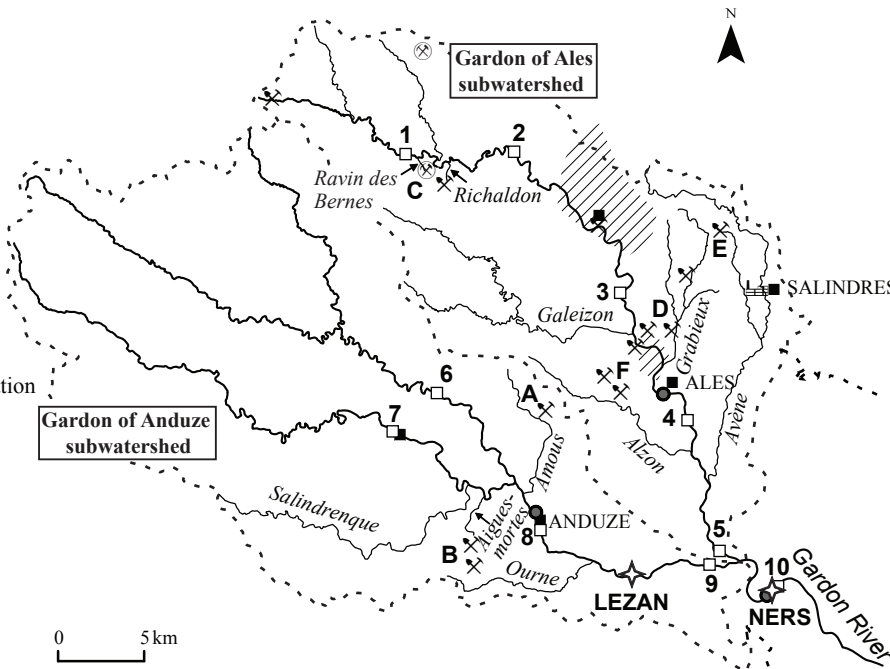
	Filtration delay	SPM mg/L	As µg/L	Cd µg/L	Pb µg/L	Sb µg/L	Tl µg/L	Zn µg/L
Ners station	t = 0	<5	5.45 ± 0.06	0.009 ± 0.002	0.234 ± 0.003	0.99 ± 0.01	0.086 ± 0.002	1.31 ± 0.09
	t = 72 h		5.1 ± 0.1	0.008 ± 0.003	0.171 ± 0.001	1.00 ± 0.02	0.094 ± 0.002	1.36 ± 0.06
Lezan station	t = 0	71	5.7 ± 0.1	0.010 ± 0.002	0.82 ± 0.01	0.57 ± 0.02	0.071 ± 0.001	3.18 ± 0.01
	t = 72 h		5.6 ± 0.2	0.010 ± 0.002	0.136 ± 0.001	0.60 ± 0.02	0.116 ± 0.001	0.28 ± 0.02

River	Watershed area (km ²)	Sample type	As	Cd	Pb	Sb	Zn	Reference
Gardon River (France)	1100	<i>Dissolved phase (µg/L)</i>	0.7-8.0 ^a	0.005-0.08 ^a	0.03-0.20 ^a	0.12-11 ^a	0.85-11 ^a	This study
			2.9-10 ^b	0.007-0.05 ^b	-	0.2-0.9 ^b	-	
		<i>SPM (mg/kg)</i>	22-87 ^a	0.28-1.0 ^a	38-138 ^a	1.9-55 ^a	145-335 ^a	
			61-1233 ^b	1.1-5.3 ^b	116-772 ^b	4.0-9.7 ^b	270-1267 ^b	
Lot River (France)	11840	<i>Dissolved phase (µg/L)</i>	-	0.01-0.27	0.05-0.32	-	3.1-17	Audry (2003) & Coynel et al. (2007) for As and Sb
		<i>SPM (mg/kg)</i>	51-95	0.26-38	14-272	2.7-18	52-2656	
Isle River (France)	6600	<i>Dissolved phase (µg/L)</i>	0.1-35	<0.002-0.22	0.01-2.8	0.4-1.1	0.53-27	Grosbois et al. (2009) & Masson et al. (2006, 2007)
		<i>SPM (mg/kg)</i>	18-109	0.79-12	32-338	-	180-2270	
Odra River (Czech Republic)	136 528	<i>Dissolved phase (µg/L)</i>	0.1-8.8	0.002-1.1	<d.l.-11	-	1.3-202	Rybicka et al. (2005)
		<i>SPM (mg/kg)</i>	2.0-302	0.9-40	9.4-1614	-	111-31369	
Tees River (UK)	1906	<i>Dissolved phase (µg/L)</i>	-	0.02-0.10	0.05-0.82	-	0.7-14	Laslett (1995)
		<i>SPM (mg/kg)</i>	-	0.6-5.4	110-320	-	190-1100	
Tamar River (UK)	1700	<i>Dissolved phase (µg/L)</i>	2.1-9.9	<d.l.	<0.46	-	3.1-28	Mighanetara et al. (2009)
Avoca River (Ireland)	652	<i>Dissolved phase (µg/L)</i>	0-0.03	0-0.61	-	-	170-640	Gray (1998)
Litavka River (Czech Republic)	630	<i>SPM (mg/kg)</i>	-	6.1-47	102-2070	-	603-3800	Žák et al. (2009)
Rhône River (France)	98800	<i>Dissolved phase (µg/L)</i>	1.2-4.7	-	0.02-0.43	0.16-0.65	0.70-8.4	Ollivier et al. (2011)
		<i>SPM (mg/kg)</i>	-	0.28-1.1	22-109	0.82-5.0	107-336	

^arange of values obtained from spatial surveys

^brange of values obtained during flood monitoring at Lezan and Ners stations

<d.l. lower than detection limit



- ✦ Autosampler station
- Manual sampling station
- Discharge monitoring station
- Town
- - - Watershed limit

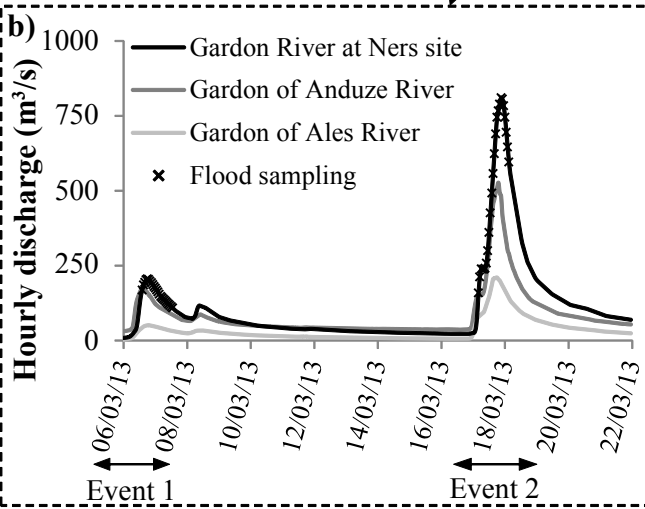
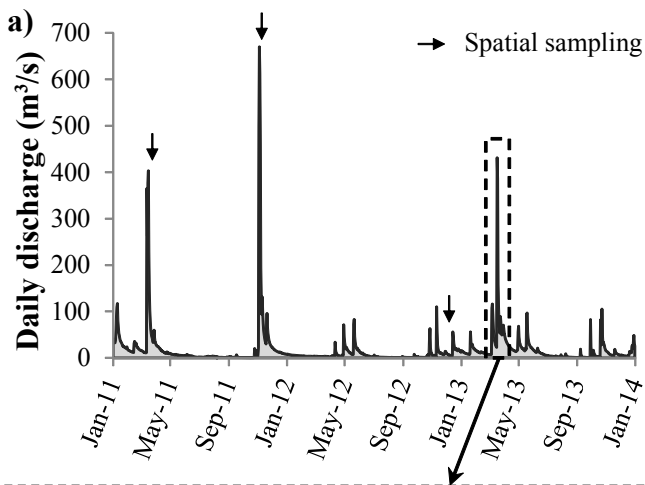
Chemical industrial center



Former mining sites

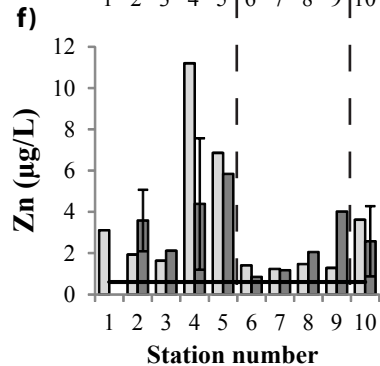
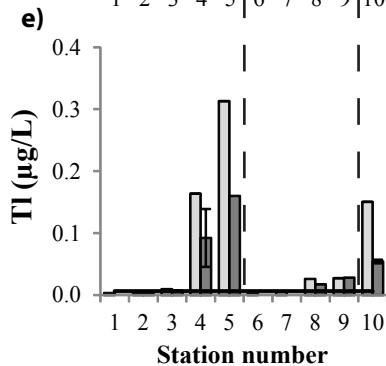
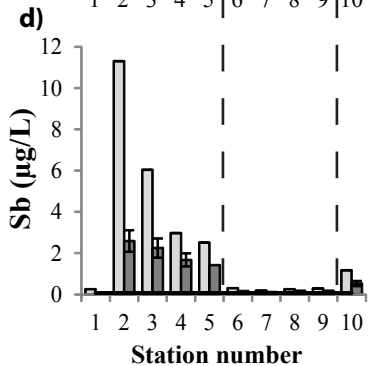
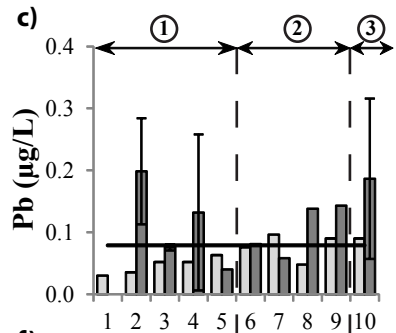
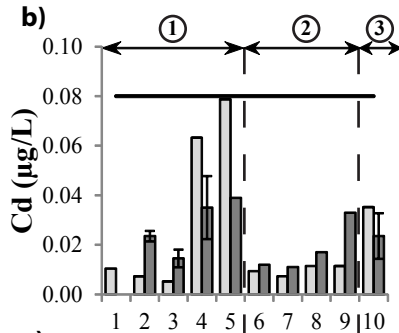
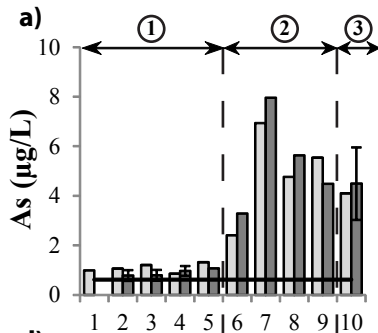
- //// Coal
- ✕ Pb/Zn
- ⊗ Sb





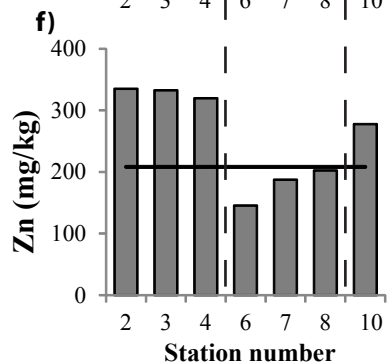
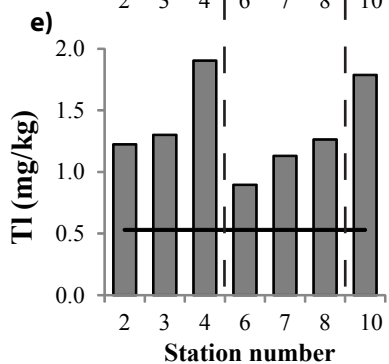
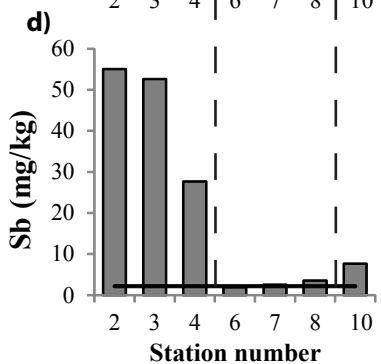
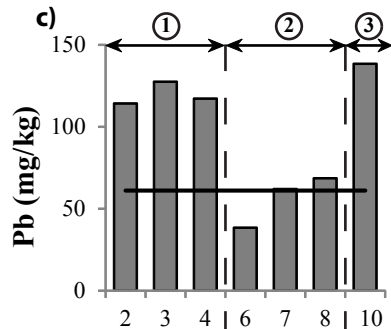
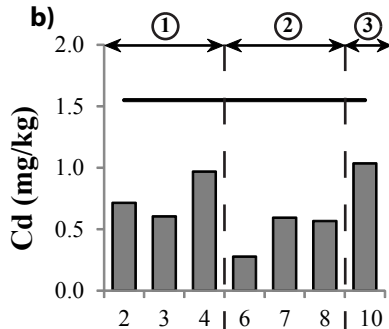
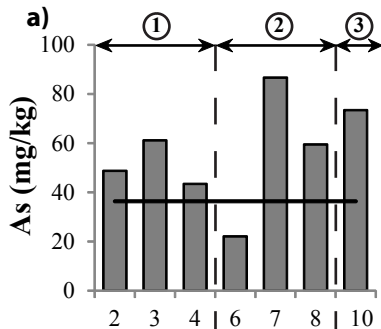
Low flow
 High flow
 World river average

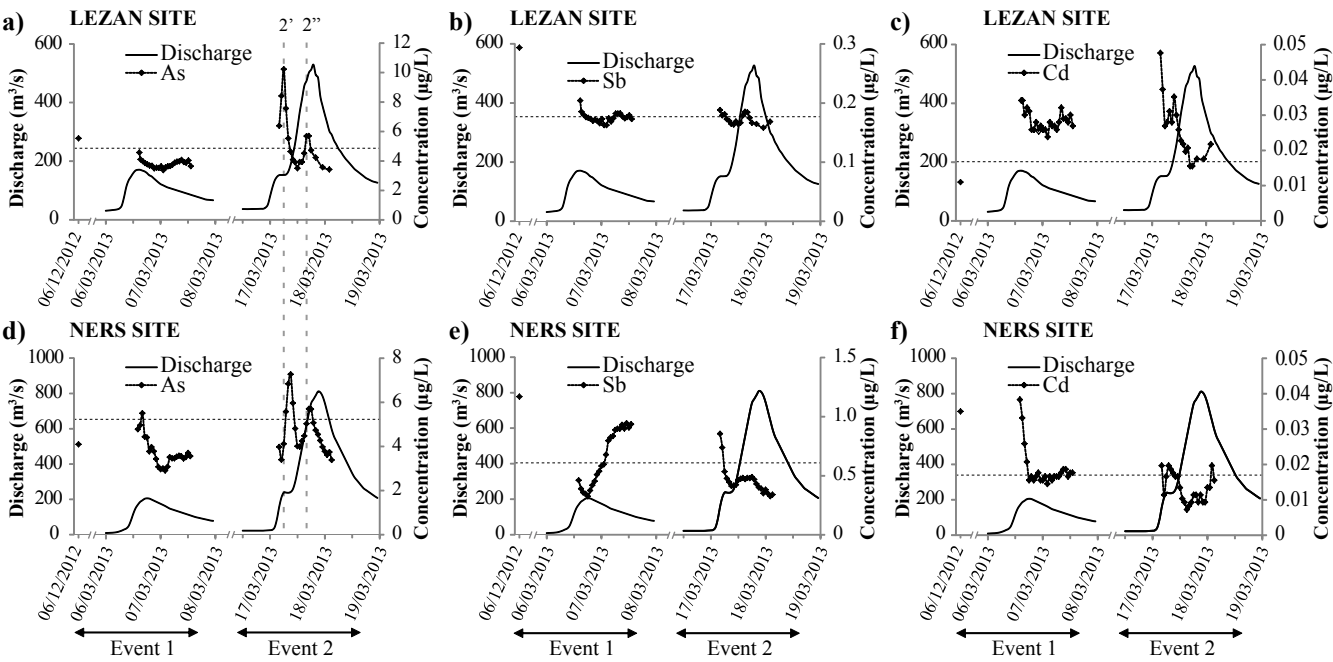
① Gardon of Ales River
 ② Gardon of Anduze River
 ③ Gardon River at Ners

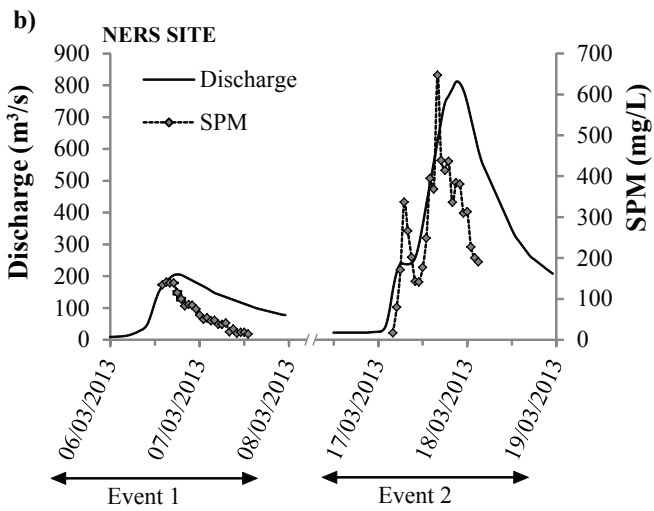
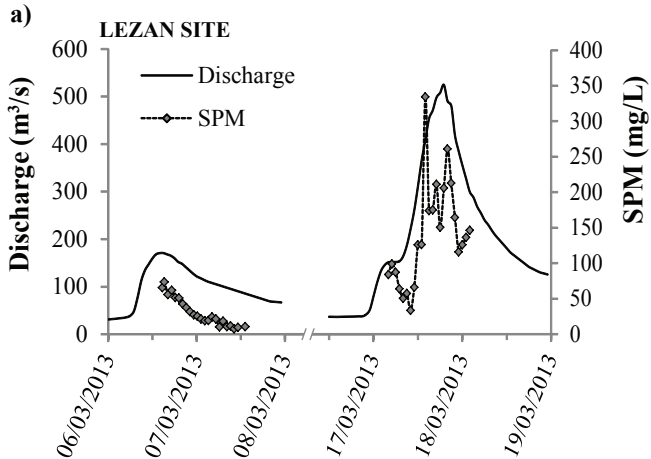


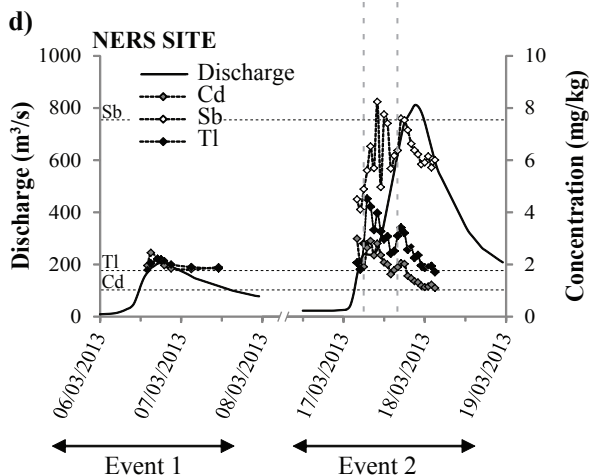
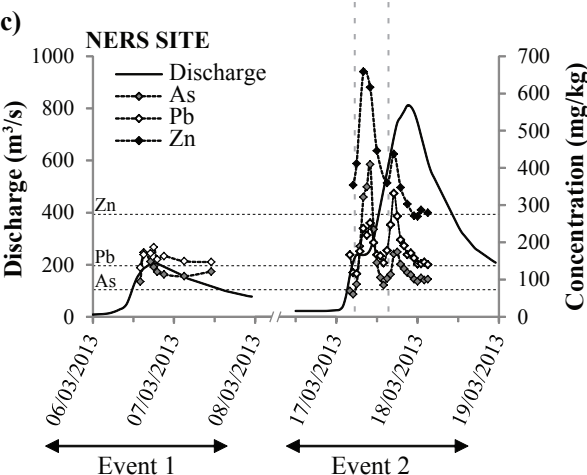
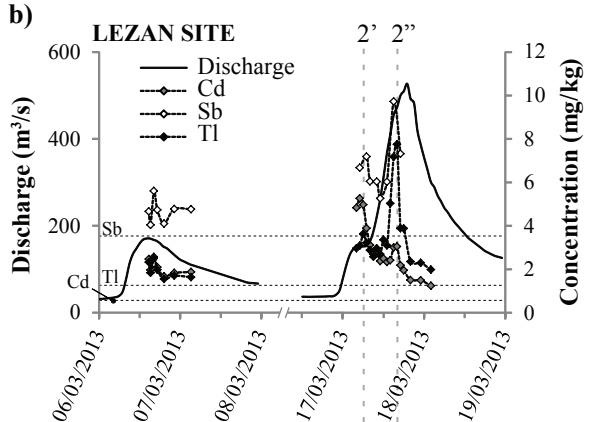
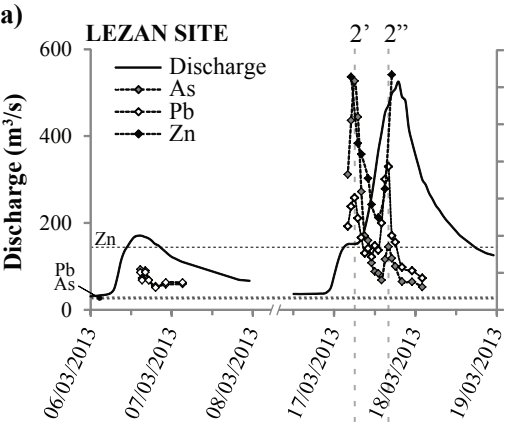
— World river average

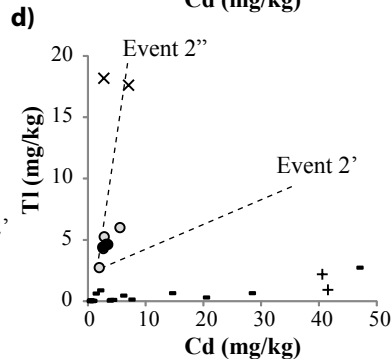
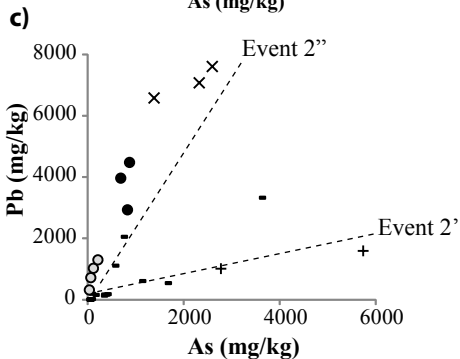
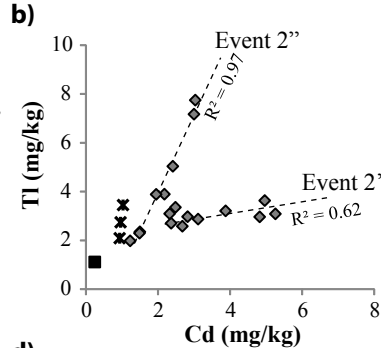
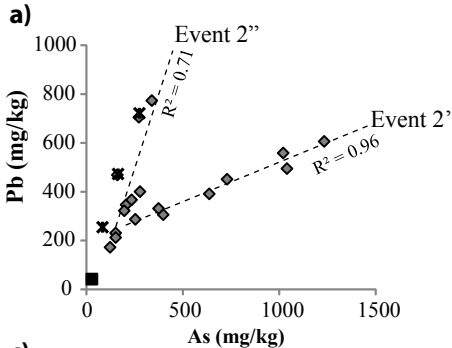
- ① Gardon of Ales River
- ② Gardon of Anduze River
- ③ Gardon River at Ners











◆ Flood samples of Event 2 at Lezan site¹

■ Local geochemical background²

✕ Flooding terrace sediments 1976-dated²

✕ Sulfide-rich tailings of the Carnoulès mine^{3,4}

**Material from the Amous River
(Carnoulès mining district):**

● Streambed bulk sediments²

- SPM (2004-2007; November 2011*)^{1,5}

+ Fine Fe-rich surface deposits*⁶

**Material from the Ourne and Aigues-
mortes Rivers (Pallières mining**

○ Streambed bulk sediments²

Supplementary Information

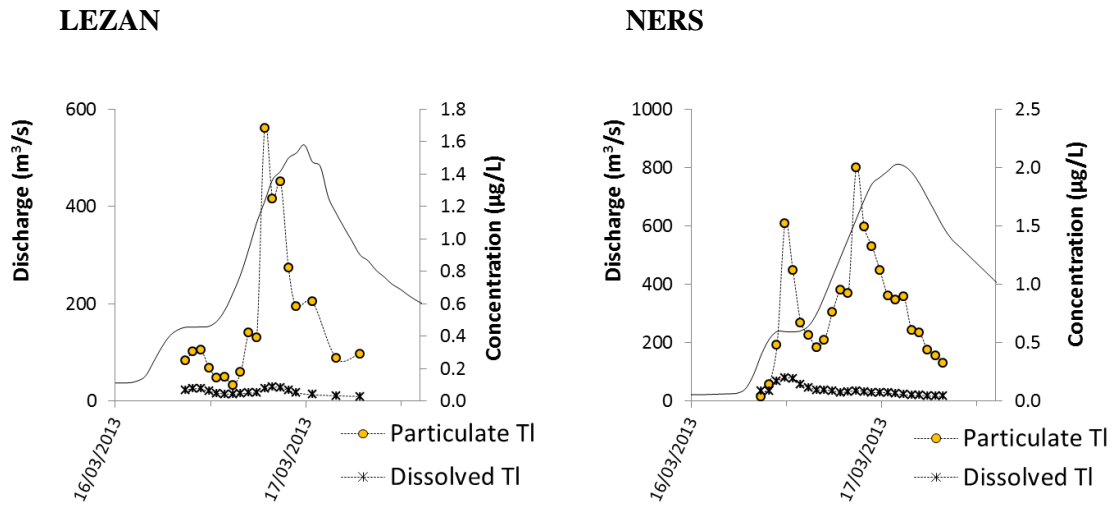


Figure 1: Variations of dissolved (black crosses) and particulate (yellow circles) TI concentrations (expressed in µg/L) during the flood event 2 (left: Lezan station; right: Ners station).

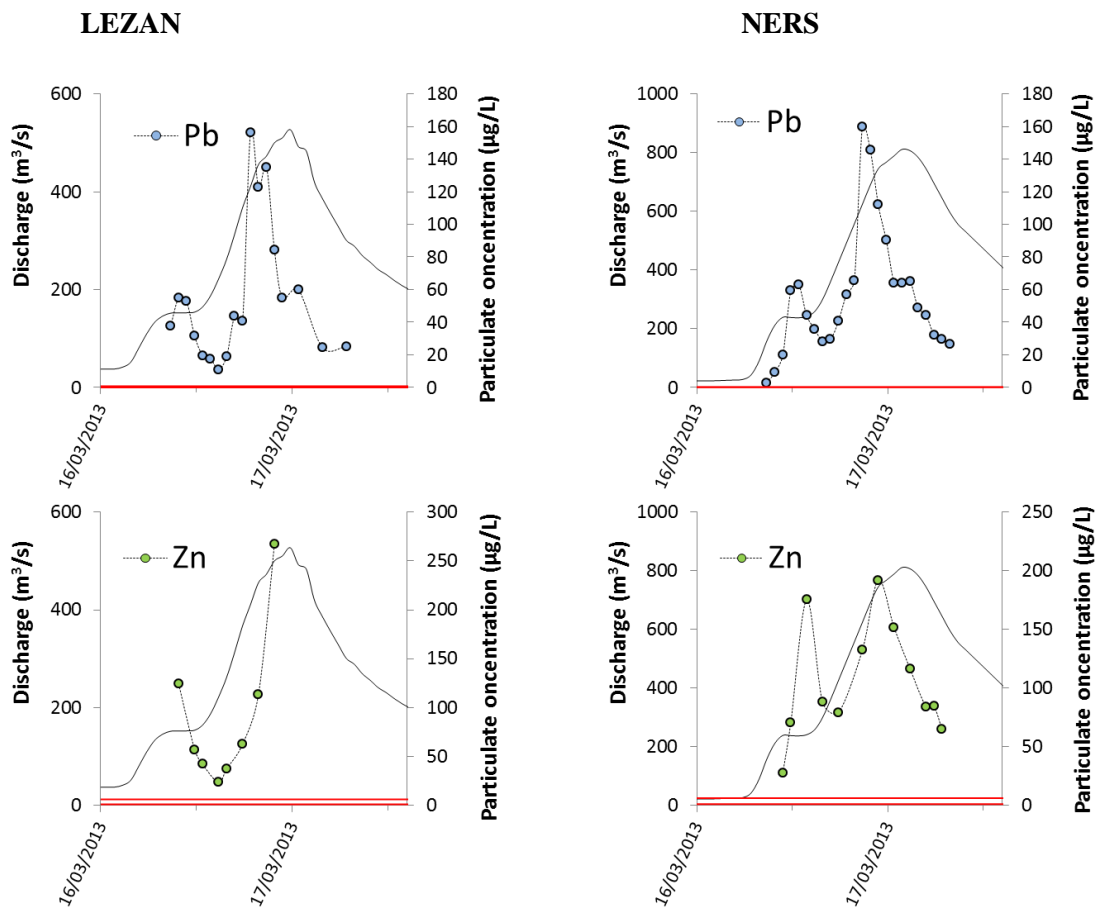


Figure 2: Variations of particulate Pb and Zn concentrations (expressed in µg/L) during the flood event 2 (left: Lezan station; right: Ners station). The red lines correspond to the minimum and the maximum dissolved concentrations obtained at both stations under different hydrological conditions after immediate filtration (Lezan n=5; Ners n=4).